HIV-1 Nef Perturbs Artificial Membranes: Investigation of the Contribution of the Myristoyl Anchor

Ruth Szilluweit,[†] Annegret Boll,[†] Sonja Lukowski,[†] Holger Gerlach,[‡] Oliver T. Fackler,[§] Matthias Geyer,[‡] and Claudia Steinem[†*]

[†]Institute of Organic and Biomolecular Chemistry, Georg-August University, 37077 Göttingen, Germany; [‡]Max Planck Institute for Molecular Physiology, 44227 Dortmund, Germany; and [§]Department of Virology, University of Heidelberg, 69120 Heidelberg, Germany

ABSTRACT Nef, an accessory protein from human immunodeficiency virus type 1, is critical for optimal viral replication and pathogenesis. Here, we analyzed the influence of full-length myristoylated and nonmyristoylated Nef on artificial lipid bilayers composed of 1-palmitoyl-2-oleoyl-*sn*-glycero-3-phosphocholine (POPC). By means of cosedimentation assays, we found that neither nonmyristoylated nor myristoylated Nef stably binds to POPC unilamellar vesicles. Time-resolved ellipsometry rather indicates that the proteins perturb the assembly of POPC planar bilayers. This observation was corroborated by fluorescence and scanning force microscopy, suggesting that membrane disordering occurs upon interaction of full-length myristoylated and nonmyristoylated Nef with planar POPC membranes immobilized on SiO_2 surfaces resulting in loss of material from the surface. The membrane perturbations were further investigated by vesicle release experiments, demonstrating that the disordering results in defects through which the fluorophor carboxyfluorescein can pass. From these results, we conclude that Nef is capable of disordering and perturbing lipid membranes and that the myristoyl group is not the decisive determinant for the action of the protein on lipid membranes.

INTRODUCTION

The human immunodeficiency virus type 1 (HIV-1) Nef protein is an N-terminally myristoylated protein of 24–32 kDa size that belongs to the so-called accessory proteins of HIV (1,2). Several functions have been attributed to Nef, which can in principle be classified into three categories: 1), alteration of cell-surface exposure of receptor molecules such as CD4 and MHC I, 2), modulation of signal-transduction pathways, and 3), enhancement of virus infectivity (as reviewed in (3–6)). Hence, in individuals infected with Nef-deficient viruses, a significantly delayed disease progression is observed (7–9).

It is supposed that the functions of Nef that mediate the alteration of signaling and trafficking pathways require its membrane association. This targeting is mediated by an N-terminal myristoylation site, which is essential for membrane attachment (10,11). Although all Nef alleles contain the highly conserved myristoylation motif, it is also observed in cellular fractionation assays from transient transfections that <40% of all Nef protein is localized at membranes, whereas the majority is found in the cytosol (11–15). It is not known whether these two populations of Nef represent a dynamic equilibrium, in which individual Nef molecules shuttle on and off the membrane or whether they are distinct biochemical species with different functions. Arold and Baur (16) speculated that after translation, Nef adopts a ''closed conformation'' to hide potential binding sites and to prevent proteolytic digestions of its flexible regions. In this conformation, the myristoyl moiety might interact with a hydrophobic region on the core domain, which could explain why the majority of the protein is localized in the cytosol and not attached to membranes. However, myristic acid is a short fatty acid (C14) and therefore forms only a weak membrane anchor when it is exposed. Accordingly, myristoylation is often not sufficient to target a protein stably into a lipid bilayer (17,18).

Here, we addressed the question of how the myristoyl anchor of HIV-1 Nef influences its interaction with lipid membranes in vitro. By means of vesicle cosedimentation assays and time-resolved ellipsometry, we studied the binding properties of wild-type (wt) Nef in comparison to the mutant Nef G2A lacking the myristoyl anchor (Fig. 1) to 1-palmitoyl-2-oleoyl-*sn*-glycero-3-phosphocholine (POPC) lipid bilayers. Unexpectedly, we observed an interaction with the membrane that was independent of the myristoylation state of Nef. Moreover, instead of stable membrane association, Nef induced membrane perturbations resulting in the detachment of lipids from the surface. To investigate this in more detail, release experiments on large unilamellar vesicles (LUVs) as well as fluorescence and scanning force microscopy imaging were performed that allowed to visualize the membrane alterations.

MATERIALS AND METHODS

Materials

POPC was purchased from Avanti Polar lipids (Alabaster, AL). Sulforhodamine 101 dihexadecanoylphosphatidylethanolamine (DHPE) was obtained from Sigma Aldrich (Taufkirchen, Germany). Fluorescein isothiocyanate (FITC)-conjugated rabbit anti-6xHIS antibody was from Dunn Labortechnik (Asbach, Germany). The silicon substrates were obtained from Si-Mat

Submitted August 28, 2008, and accepted for publication December 30, 2008.

*Correspondence: claudia.steinem@chemie.uni-goettingen.de

Editor: Peter Hinterdorfer.

0006-3495/09/04/3242/9 $2.00

doi: 10.1016/j.bpj.2008.12.3947

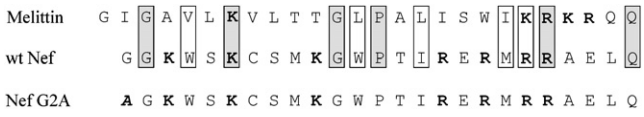

FIGURE 1 Amino acid sequences of melittin and the N-terminus of full-length HIV-1 wt Nef and the corresponding mutant Nef G2A. Identical residues of melittin and wt Nef are shown in shaded boxes, and analogous residues are marked in open boxes. Basic residues are highlighted in bold.

(Landsberg/Lech, Germany) and from CrysTec (Berlin, Germany). The Sephadex G-25 column was purchased from Biotech AB (Uppsala, Sweden). Water was purified first through a Millipore water-purification system Milli-RO 3 plus and finally with a Millipore ultrapure water system Milli-Q plus 185 (specific resistance = 18.2 MΩ/cm) (Billerica, MA).

Protein preparation

Myristoylated wt Nef protein, HIV-1 allele SF2 (AC:K02007), was prepared in *Escherichia coli* BL21(DE3) cells from a codon optimized plasmid by coexpression with the *N*-myristoyl transferase and addition of myristic acid as substrate, similarly as described (19). The protein contained a C-terminal hexahistidine tag for purification by nickel affinity chromatography. Nonmyristoylated Nef G2A was polymerase chain reaction-amplified with *Nco*I/*Hind*III restriction sites and cloned into the pET-23d expression vector (Novagen) and expressed without the *N*-myristoyl transferase. The accuracy of all plasmid constructs was confirmed by nucleotide sequencing. Full myristoylation was confirmed by ESI analytical mass spectrometry. All proteins were concentrated to ~10 mg/ml in 20 mM Tris/HCl buffer (pH 8) with 50 mM NaCl, 1 mM DTE, aliquoted, shock frozen, and stored at −80°C.

Vesicle preparation

Lipid films composed of POPC or POPC doped with 0.1 mol % sulforhodamine 101 DHPE were prepared at the bottom of glass test tubes by drying the lipids dissolved in chloroform under a stream of nitrogen while heating above 30°C followed by 3 h under vacuum. The lipid films were stored at 4°C. To obtain multilamellar vesicles, a lipid film was incubated in buffer solution (20 mM Tris/HCl, 100 mM NaCl, pH 7.4) for 30 min followed by vortexing it three times for 30 s every 5 min. The resulting multilamellar vesicles were converted into LUVs by the extrusion method using a polycarbonate membrane with a pore diameter of 100 nm (20).

For release measurements, multilamellar vesicles were prepared as mentioned above, but the buffer solution contained additional 100 mM 5(6)-carboxyfluorescein (CF). After formation of LUVs, the external fluorescence dye was removed from the vesicles by gel filtration using a Sephadex G-25 column.

Preparation of solid-supported membranes on SiO_2 surfaces

First, the silicon substrates were cleaned with isopropanol and ultrapure water. Then, they were incubated in an aqueous solution of NH_3 and H_2O_2 (5/1/1 $H_2O/NH_3/H_2O_2$) for 15 min at 70°C. Finally, the substrates were rinsed with ultrapure water.

For preparation of solid-supported membranes on silicon dioxide, the well-known technique of spreading and fusion of unilamellar vesicles on hydrophilic surfaces was used as described (21–23). For fluorescence and scanning force microscopy images, the substrates were placed in an open Teflon cell and incubated with the vesicle suspension (0.05 mg/mL) for 1 h at room temperature. Remaining vesicles were removed by rinsing the surface with a buffer flow (20 mM Tris/HCl, 100 mM NaCl, 1 mM dithiothreitol (DTT), pH 7.4).

For ellipsometry experiments, the silicon substrates were placed in a fluid cell (Nanofilm Technologie, Göttingen, Germany). The cell was filled with buffer solution (20 mM Tris/HCl, 100 mM NaCl, pH 7.4), and POPC vesicles (0.2 mg/mL) were continuously pumped through the cell by a peristaltic pump with a velocity of 0.5 mL/min for 1 h at room temperature. The remaining vesicles were removed by rinsing the cell with buffer solution (20 mM Tris/HCl, 100 mM NaCl, 1 mM DTT, pH 7.4) for 30 min.

Vesicle cosedimentation assay

Freshly prepared LUVs (0.5 mg/mL) were incubated at 4°C overnight with HIV-1 wt Nef and HIV-1 Nef G2A, respectively. Lipid/protein of 365:1 and 65:1 was chosen. Then, the LUVs were centrifuged at 4°C and 232,000 × *g* for 1 h, and a sample was taken from the supernatant. After the supernatant was carefully removed, the vesicle pellet was redissolved in buffer (20 mM Tris/HCl, 100 mM NaCl, pH 7.4) and centrifuged at 4°C and 232,000 × *g* for 1 h. Samples were taken from the supernatant and the pellet. All samples were treated with 0.175 M Tris/HCl, 5% SDS (w/v), 15% glycerol (v/v), 0.06 g/L bromphenol blue, and 0.3 M DTT at pH 6.8 and heated for 5 min at 95°C. Equivalent amounts of the supernatant fractions and the pellet were analyzed with sodium dodecyl sulfate-polyacrylamide gel electrophoresis (SDS-PAGE). The SDS-polyacrylamide gels (17%) were stained with Coomassie brilliant blue.

Ellipsometry

Ellipsometry is a well-known technique for the characterization of thin films (24–27). To observe a change in membrane film thickness as a result of membrane-protein interactions, experiments were carried out using a Nanofilm EP^3 ellipsometer (Nanofilm Technologie, Göttingen, Germany). The instrument was equipped with a laser emitting at a wavelength of 636.7 nm. The angle of incidence was set to 60°. The resulting ellipsometric angles delta and psi were recorded as a function of time using the one zone nulling procedure. The membrane film thickness was calculated based on a model composed of bulk silicon followed by silicon dioxide, on which a lipid bilayer was deposited. The refractive indices for doped silicon, silicon dioxide, and water were taken from a database included in the software (LayTec, Berlin, Germany). The refractive index for water was applied for the buffer solution, as the low salt concentration does not significantly influence the refractive index. The refractive index for a lipid bilayer was taken from literature (27).

Fluorescence microscopy

For fluorescence microscopy, planar POPC membranes were doped with 0.1 mol % sulforhodamine 101 DHPE. After addition of protein and incubation overnight at 4°C, the samples were rinsed with buffer solution, and fluorescence images were taken using an AxioTech Vario (Zeiss, Göttingen, Germany) fluorescence microscope equipped with a 40× or 63× water immersion objective (ACHROPLAN, na = 0.8 water, Zeiss, Hamburg, Germany). To follow the fluorescence of sulforhodamine 101 DHPE the filter set 45 (Zeiss, Göttingen, Germany) and of FITC-conjugated rabbit anti-6xHIS antibody the filter set 44 (Zeiss, Göttingen, Germany) was used.

Scanning force microscopy

Scanning force microscopy was performed using a JPK NanoWizard II scanning force microscope (JPK Instruments, Berlin, Germany). All images were obtained in aqueous solution in contact mode using silicon cantilevers (CSC 38) from Ultrasharp (Moscow, Russia) with a nominal spring constant of 0.03 N/m with a typical scan rate of 0.5 Hz and a scan angle of 90°. Image resolution was 512 × 512 pixels.

CF release from lipid vesicles

CF release from LUVs composed of POPC was followed by monitoring the increase of the fluorescence signal $F(t)$ as a function of time after the addition of HIV-1 wt Nef and HIV-1 Nef G2A. All experiments were performed with a fluorometer (FP 6500 Jasco, Gotha, Germany). CF fluorescence was

measured using an excitation wavelength of 490 nm (slit width: 5 nm) and an emission wavelength of 520 nm (slit width: 5 nm). The maximum fluorescence intensity signal F_t was determined after the addition of 2 μL Triton X-100 (10% (w/w)) to a total volume of 600 μL, which destroys the vesicles. The normalized fluorescence F_{rel} defined as (Eq. 1):

$$F_{rel}(t) = \frac{F(t) - F_0}{F_t - F_0} \quad (1)$$

is plotted as a function of time, with F_0 being the fluorescence intensity before the addition of protein. All measurements were performed in 20 mM Tris/HCl, 100 mM NaCl, 1 mM DTT, pH 7.4 at room temperature.

RESULTS

Interaction of HIV-1 Nef with lipid vesicles

It is thought that the biological activities of Nef require its association with cellular membranes and that this interaction is mediated by its N-terminal myristoylation. To investigate whether myristoylation is the only requirement for membrane association in vitro, we performed cosedimentation assays using LUVs. POPC-LUVs were incubated with HIV-1 Nef wt and HIV-1 Nef G2A, which lacks the myristoyl acceptor glycine at position 2 and therefore is not myristoylated. After centrifugation of the vesicles, the supernatants and pellets were analyzed by SDS-PAGE (Fig. 2). HIV-1 wt Nef as well as HIV-1 Nef G2A were only found in the supernatants (S1, lanes 2 and 5), whereas no protein was detected in the vesicle pellet. This suggests that a strong interaction of the protein to the membrane does not occur irrespective of the presence of the myristic acid moiety. Because it has been proposed that a subpopulation of Nef resides in detergent-resistant membrane microdomains or lipid rafts (15,28–30), we performed the same experiment with a lipid mixture that resembles rafts, namely POPC/sphingomyelin/cholesterol in a 2:1:1 ratio. However, a similar result as for POPC-LUVs was obtained; neither wt Nef nor Nef G2A was found in the vesicle pellet (Fig. 2 *B*), suggesting that no stable interaction between the protein and the lipid bilayer takes place.

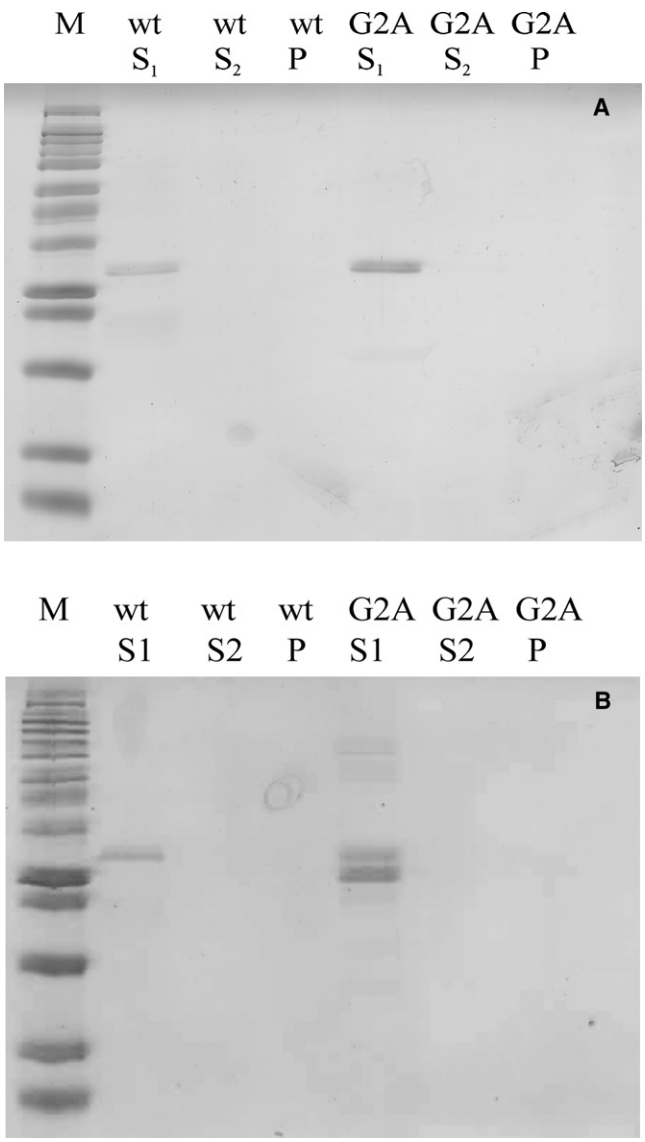

FIGURE 2 SDS-PAGE analysis of the cosedimentation assays of POPC-LUVs and either HIV-1 wt Nef (wt) or HIV-1 G2A (G2A) (*A*). Panel *B* shows the result of an SDS-PAGE analysis of the cosedimentation assay of POPC/sphingomyelin/cholesterol 2:1:1 LUVs and either HIV-1 wt Nef (wt) or HIV-1 G2A (G2A). Proteins were visualized by Coomassie staining. M, protein marker; S_1, supernatant; S_2, supernatant after washing; and P, pellet.

Interaction of HIV-1 Nef with planar bilayers

As the vesicle cosedimentation assay only shows the amount of protein stably bound to the membranes, we next used planar lipid bilayers on silicon substrates. These membranes allow for the detection of protein binding in a time-resolved manner by monitoring changes in thickness by means of ellipsometry. First, LUVs composed of POPC were spread on silicon dioxide surfaces. The bilayer formation process was observed by measuring the changes of the ellipsometric angles delta and psi as a function of time (data not shown). From delta and psi, the membrane film thickness was calculated using the software LayTec. A mean lipid bilayer thickness of (6.3 $\pm$ 0.8) nm ($n = 12$) was obtained. The value demonstrates the formation of planar POPC bilayers on the silicon substrates. After the bilayer had been established, 0.5 μM HIV-1 wt Nef and 0.5 μM HIV-1 Nef G2A, respectively, were added and continuously pumped through the cell by a peristaltic pump with a velocity of 0.5 mL/min for 1 h at room temperature, followed by rinsing the sample with buffer solution for 30 min to remove nonbound protein.

Surprisingly, in none of the experiments an increase in film thickness upon addition of the protein was monitored, suggesting that protein binding to the membrane does not occur or that it occurs only transiently. Instead, a decrease in film thickness was observed after protein addition. Two typical time courses of the change in membrane film thickness after the addition of HIV-1 wt Nef and HIV-1 Nef G2A are depicted in Fig. 3. The addition of HIV-1 wt Nef

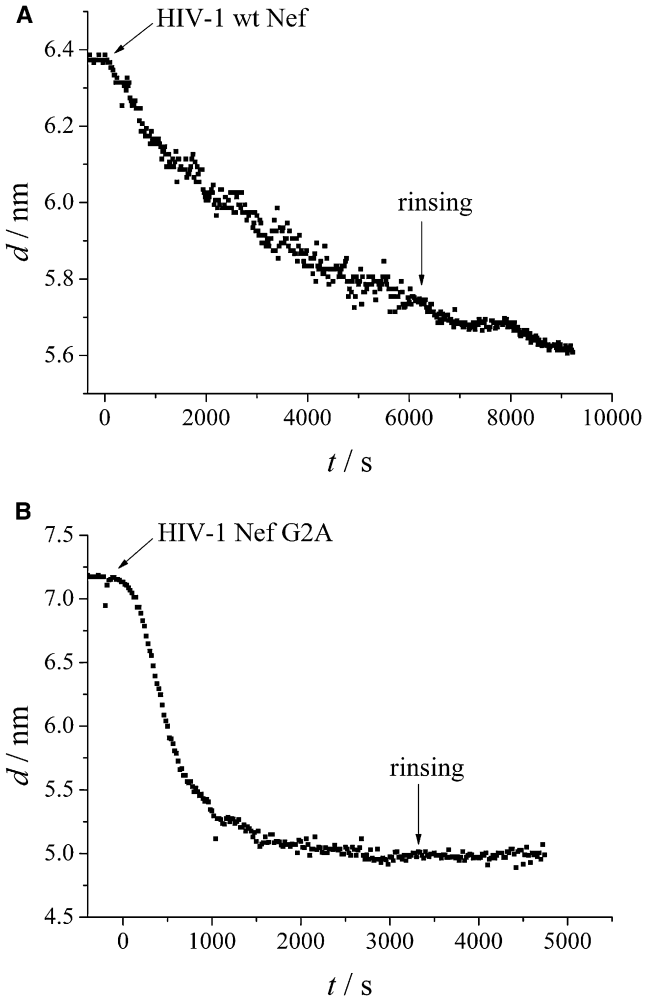

FIGURE 3 Ellipsometry measurements showing the change of POPC membrane thickness after addition of 0.5 μM HIV-1 wt Nef (*A*) and 0.5 μM HIV-1 Nef G2A (*B*) and rinsing with buffer solution. The time point of addition of the protein is marked as $t = 0$.

(Fig. 3 *A*) resulted in a decrease in membrane thickness by 9.0% after the addition of the protein. Rinsing with buffer solution decreased the membrane thickness further by ~2.1%. On average, a decrease in membrane thickness of (9 ± 4)% was observed (Table 1). Immediately after the addition of HIV-1 Nef G2A (Fig. 3 *B*), the film thickness decreased by 29.1%. No further decrease in thickness was observed after rinsing with buffer solution. From five independent measurements, an average change in membrane thickness of (30 ± 7)% was observed (Table 1). We attribute this decrease in membrane thickness to a destabilization of the lipid bilayer presumably resulting in a detachment of lipids from the silicon dioxide surface upon interaction with myristoylated and nonmyristoylated Nef.

TABLE 1 Average decrease in membrane film thickness after the addition of HIV-1 Nef

Protein	Decrease in film thickness (%)
HIV-1 wt Nef	9 ± 4 ($n = 7$)
HIV-1 Nef G2A	30 ± 7 ($n = 5$)

Visualization of membrane disordering by fluorescence microscopy

To get further information about the lipid destabilization process and to visualize a possible lipid detachment from the surface, we used fluorescence in conjunction with scanning force microscopy on planar lipid membranes composed of POPC immobilized on silicon dioxide surfaces. For a fluorescence inspection of the formed membranes, they were doped with 0.1 mol % sulforhodamine 101 DHPE. A homogeneous fluorescence as shown in Fig. 4 *A* indicates a complete bilayer with no defects. Only to defect-free POPC-bilayers Nef protein was added. HIV-1 wt Nef was added at different concentrations under flow and static conditions (see the Supporting Material). Incubation at a final concentration of 1.0 μM and rinsing with buffer solution to remove nonbound protein from solution results in the fluorescence images as shown in Fig. 4 *C*. A nonhomogeneous fluorescence became discernable with a large number of black spots.

To rule out that the membrane changed its appearance as a result of the incubation time, the same experiment was performed without addition of HIV-1 wt Nef as control (Fig. 4 *B*). No inhomogeneity of the fluorescence signal was observed even after 14 h incubation time. To investigate if protein is localized in the dark areas, where fluorescently labeled lipids are no longer present or if these areas are free of lipid and protein, the sample was incubated with FITC-conjugated rabbit anti-6xHIS antibody (1:250) for 2 h at room temperature. After rinsing with buffer solution to remove nonbound antibody, fluorescence images were taken (Fig. 4 *D*). An almost perfect overlay of the nonfluorescent regions in the membrane and the positions of the antibody (compare Fig. 4, *C* and *D*) was found suggesting the presence of Nef. In a similar set of experiments the influence of HIV-1 Nef G2A on planar POPC membranes immobilized on silicon dioxide was investigated. Similar results were obtained (Fig. 5). After incubation of the membranes with HIV-1 Nef G2A, black spots appeared in the membrane indicative of its destabilization and disordering. Incubation with the FITC-conjugated rabbit anti-6xHIS antibody (1:250) resulted in a fluorescence labeling of the areas of the dark spots. The average size of these dark spots ranged from 1 to 5 μm.

Control experiments, in which the antibody was added to a pure POPC bilayer, did not show any nonspecific binding of the antibody to POPC (data not shown). Also, the addition of a nonspecific FITC labeled antibody did not result in a significant fluorescence (see the Supporting Material) as observed in the case of the specific antibody. Only a faint fluorescence was observed, which does not match the nonfluorescent regions in the membranes. From these experiments, we conclude that the interaction of the FITC-conjugated rabbit

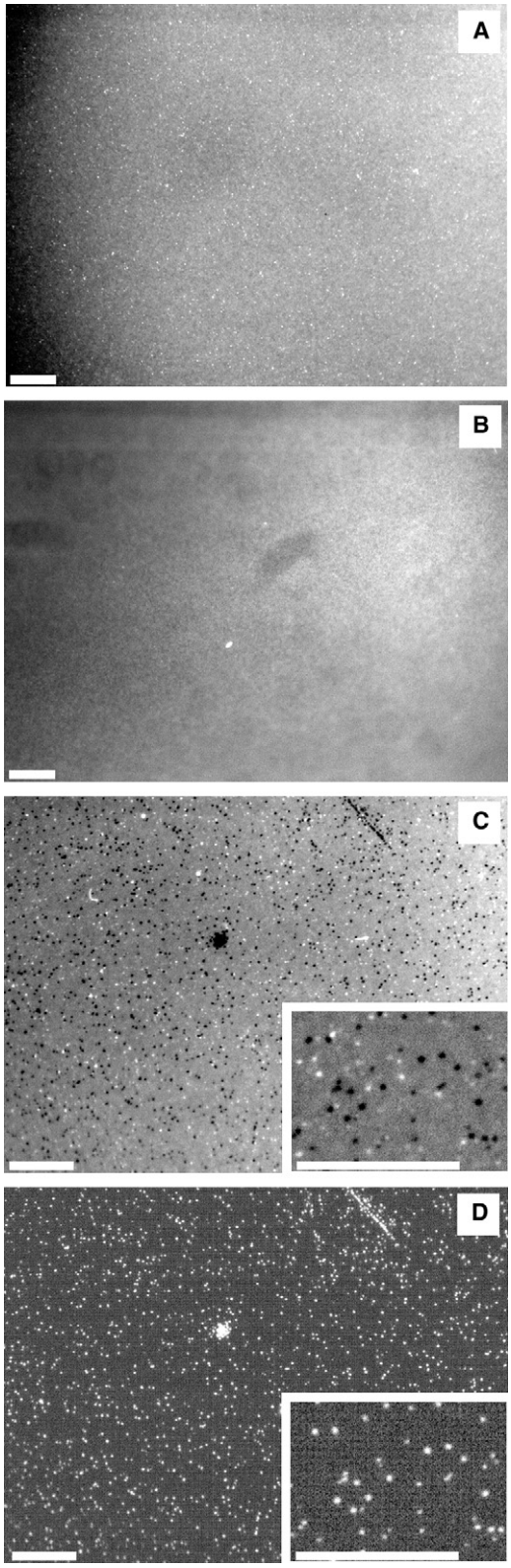

FIGURE 4 Fluorescence micrographs of a sulforhodamine 101 DHPE-doped POPC membrane. (*A*) Membrane before the addition of HIV-1 wt Nef. (*B*) Control, in which the membrane was incubated overnight at 4°C without adding protein. (*C*) Membrane after the addition of 1.0 μM HIV-1 wt Nef and incubation overnight at 4°C. (*D*) Fluorescence micrograph after the addition of FITC-conjugated rabbit anti-6xHIS antibody (1/250) and incubation for 2 h at room temperature. The insets show magnifications of the corresponding figure. All scale bars are 20 μm.

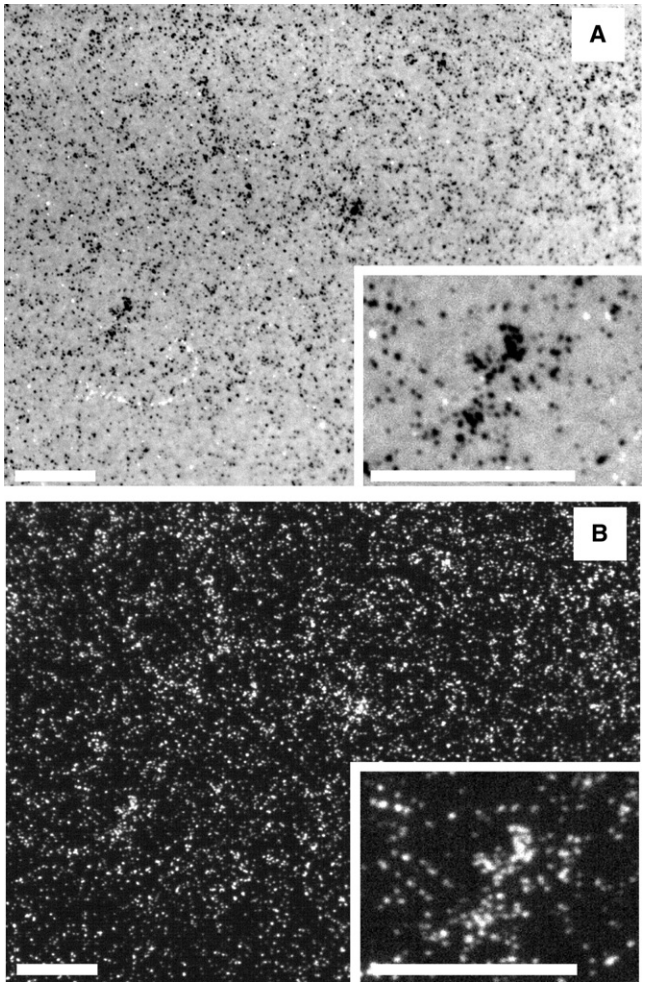

FIGURE 5 Fluorescence micrographs of a sulforhodamine 101 DHPE-doped POPC membrane. (*A*) Membrane after the addition of 1.0 μM HIV-1 Nef G2A and incubation overnight at 4°C. (*B*) Fluorescence micrograph after the addition of FITC-conjugated rabbit anti-6xHIS antibody (1:250) and incubation for 2 h at room temperature. The insets show magnifications of the corresponding figure. All scale bars are 20 μm.

anti-6xHIS antibody is specific for Nef and does not interact nonspecifically with the perturbed membrane structures.

Visualization of membrane disordering by scanning force microcopy

To obtain a higher resolution of the observed disordered membrane structures, scanning force microscopy images of the same POPC bilayers that were inspected by fluorescence microscopy were taken before and after 1.0 μM HIV-1 Nef was added. Before the addition of protein, a homogeneous membrane was visualized without any apparent perturbation of its surface texture (data not shown). After the lipid bilayer was incubated with the protein and unbound protein was

removed by rinsing the samples with buffer solution, the topography of the bilayers had considerably changed. Fig. 6, *A* and *B*, shows the topography of the bilayer after addition of HIV-1 wt Nef. Brighter areas are discernable, which are similar in size and frequency as the black spots observed in fluorescence microscopy of the same sample. The higher structure unambiguously indicates that protein is located within these areas. Similar results were obtained for HIV-1 Nef G2A (Fig. 6, *C* and *D*). The membrane surface was covered with round domains with a slightly higher topography. In general, the membranes appeared soft and were, due to their softness, difficult to image. There was no dependence of the distribution and appearance of the disordered membrane structures on whether wt or G2A Nef was used (see the Supporting Material).

Release of CF induced by HIV-1 Nef

From the obtained results, we conclude that HIV-1 Nef interacts with POPC membranes in such that it disturbs the organization of the lipid bilayers eventually resulting in the detachment of lipids from a solid substrate as described above. To address whether the perturbation of the membrane induced by the action of HIV-1 Nef results in holes through which molecules can pass, release-experiments using CF filled LUVs were performed. The CF release method has been shown to be well suited to study the formation of holes in vesicles induced by peptides and proteins (31–34). It relies on the self-quenching of encapsulated CF. When a pore forms in a vesicle containing internal CF, its release is detected as an increase in fluorescence intensity. The fluorescence signal of CF was measured at a wavelength of 520 nm in a time-resolved manner. After a stable baseline was reached, HIV-1 wt Nef was added to the vesicle suspension resulting in molar lipid/protein of 65:1. The maximum fluorescence intensity was obtained by disrupting the vesicles by adding Triton X-100. Fig. 7 *A* shows a characteristic increase of the fluorescence signal upon addition of HIV-1 wt Nef to POPC LUVs. After the addition of HIV-1 wt Nef, an increase of 14.7% of the fluorescence signal was observed indicating that some vesicles became leaky, thus releasing the fluorophor. To investigate the influence of the myristic acid moiety on the lipid perturbation, the same experiment was performed with HIV-1 Nef G2A. In this case, 22.7% of the entrapped dye was released. On average, a dye release of $(12 \pm 4)\%$ was observed for HIV-1 wt Nef, whereas for HIV-1 Nef G2A the average increase of the fluorescence signal amounted to $(14 \pm 4)\%$ (Table 2). From these results, it can be concluded that the myristoylation is not the decisive parameter for the formation of holes through which the dye can pass.

DISCUSSION

In this study, we investigated the influence of full-length Nef from HIV-1 on lipid membranes with emphasis on the impact

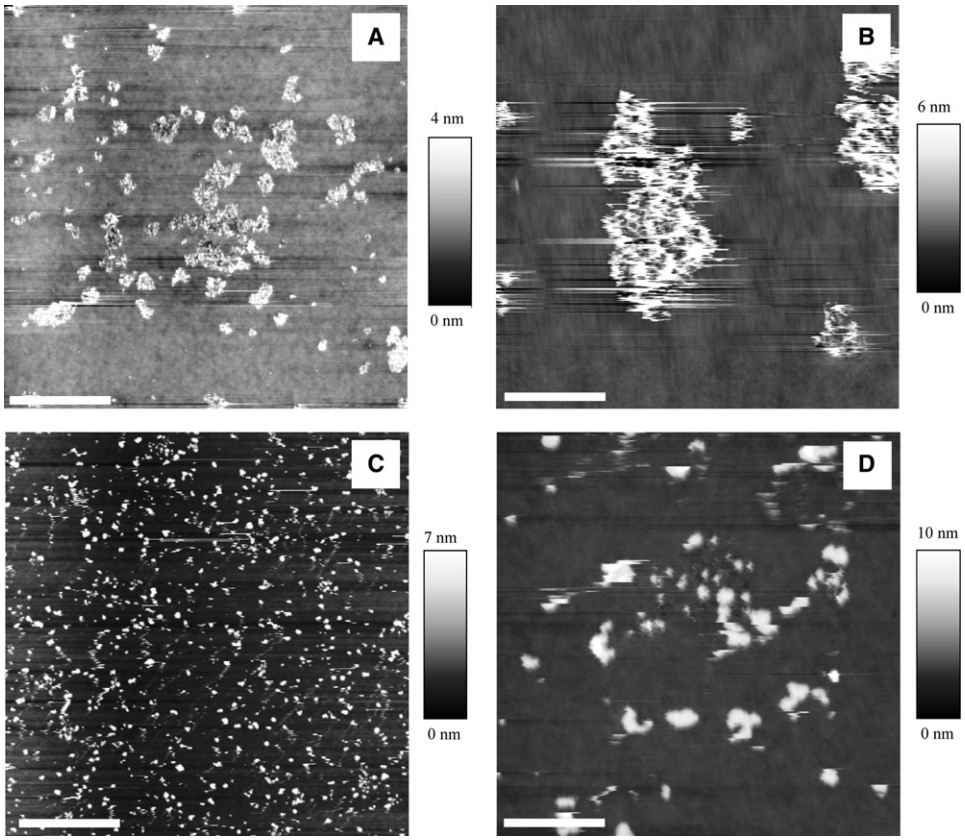

FIGURE 6 Scanning force microscopy images showing the topography (contact mode) of a POPC membrane attached to a silicon dioxide surface after the addition of 1.0 μM HIV-1 wt Nef (*A* and *B*) and 1.0 μM HIV-1 Nef G2A (*C* and *D*) Scale bar: *A* and *C*, 5 μm; *B* and *D*, 1 μm.

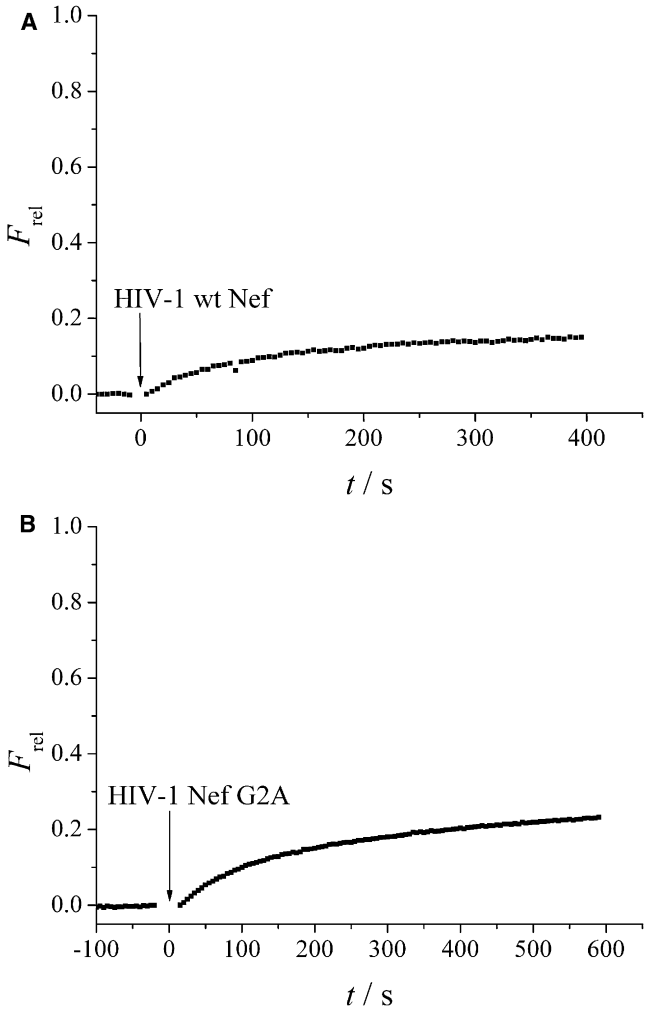

FIGURE 7 Release of CF from POPC vesicles as a function of time after the addition of HIV-1 wt Nef (*A*) and HIV-1 Nef G2A (*B*). Lipid/protein of 65:1 was used. The fluorescence signal has been normalized according to Eq. 1. Protein has been added at $t = 0$.

of its myristoyl modification. By means of vesicle cosedimentation assays, the binding ability of myristoylated HIV-1 wt Nef and the nonmyristoylated mutant Nef G2A to membranes was elucidated. Surprisingly, no stable binding to membranes was monitored even in the presence of the myristoyl anchor. This was corroborated by time-resolved ellipsometry measurements on lipid bilayers attached to silicon dioxide surfaces. Instead, both proteins perturb the membranes, which results in a decrease in membrane thickness. This decrease might result from a net loss of material, i.e., removal of lipids, from the surface (see Fig. 3). The overall amount of released material, however, cannot be quantified, as in the areas, where no lipids are present, Nef protein is found (Figs. 4–6), which is discussed in more detail below.

TABLE 2 Average increase of the fluorescence signal after the addition of HIV-1 Nef to POPC LUVs with lipid/protein of 65:1

Protein	Increase of the fluorescence signal (%)
HIV-1 wt Nef	12 ± 4 ($n = 20$)
HIV-1 Nef G2A	14 ± 4 ($n = 20$)

Earlier experiments by Curtain et al. (35) using nonmyristoylated Nef already suggested membrane perturbations. In this previous study, light-scattering as well as membrane-fusion experiments were performed. Lipid mixing was observed as well as an increase in light scattering indicating disturbance of the vesicle structure if N-terminal peptides of Nef and nonmyristoylated Nef interacted with lipid vesicles. However, all experiments were performed with small unilamellar vesicles composed of 1,2-dipalmitoyl-*sn*-glycero-3-phosphocholine, which are in the gel state at room temperature and thus are nonphysiological. In cellular experiments, Fujii et al. (36) found that the addition of recombinant, nonmyristoylated HIV-1 Nef at low concentrations inhibits the growth of CD4+ cells, whereas it leads to cell death at higher concentrations. Short N-terminal HIV-1 Nef fragments composed of at least the first 22 amino acids added to yeast and bacterial cells turned out to be cytotoxic (37,38). The addition of a myristoylated N-terminal fragment to yeast cells results in total loss of colony formation, whereas the addition of a nonmyristoylated fragment results in only 80% loss. These observations were discussed in terms of a Nef-induced membrane disruption, which results in loss of membrane into the extracellular media. All conclusions are corroborated by the sequence similarity (Fig. 1) of the N-terminus of wt Nef and melittin, a highly membrane active peptide (39). The decrease in membrane thickness as monitored by ellipsometry as well as the membrane perturbations observed by fluorescence and scanning force microscopy observed in this study confirms and extends these findings, as it reveals that lipids get disordered by full-length Nef, presumably leading to their detachment from the solid substrate. Membrane perturbations result in the exposure of the silicon dioxide surface and hydrophobic regions of the membrane leading to a different ''artificial'' adsorption site for the protein. These adsorption sites are not created in lipid vesicles, because, first, no underlying silicon dioxide is present, and, second, the perturbations are probably less stable in vesicles than on solid support, which explains why no protein cosediments with POPC vesicles are found (see Fig. 2).

We merely observed differences in the action of wt HIV-1 Nef and Nef G2A lacking the myristoyl anchor for their interaction with pure POPC bilayers. Although the myristoylation motif MGxxxS is almost totally conserved in all HIV-1 Nef alleles from different subtypes and stages of disease (1), the role of Nef myristoylation is discussed controversially in the literature. Early reports indicated that the N-terminal myristoylation of HIV-1 Nef is required for membrane association and biological activity of the protein (10,11,13,40,41). More recently, evidence has been presented that also nonmyristoylated Nef can retain considerable membrane association and functionality (14,42). In principle, it has been shown that a single myristoyl moiety is not sufficient to stably anchor a protein to the plasma membrane (17,18,43). Small

myristoylated peptides bind to a phospholipid bilayer with unitary Gibbs free binding energy of ~8 kcal/mol, which corresponds to an effective dissociation constant of only 10^{-4} M (44). Further energy contributions need to be provided to stabilize the membrane-protein association such as electrostatic interactions. At the N-terminus of Nef, the propensity of a helix is found within the arginine-rich region (arginines 17, 19, 21, 22), and this cluster of basic amino acids facilitates the targeting of the protein to the plasma membrane and stabilizes the interaction with membranes (14,45,46). It is also known that the N-terminal helical region of Nef associates with a protein complex containing Lck and a serine kinase (16,47). These interactions with membrane-associated proteins might additionally stabilize the membrane-protein interaction in vivo.

Instead of protein binding, we found that Nef is capable of disordering and perturbing the membrane assembly and that the myristoyl group is not the only decisive determinant for the action of the protein on lipid membranes. It has been previously observed that the native myristoylated Nef protein appears more compactly folded than its nonmyristoylated variant, suggesting that the myristate associates with the core domain structure of Nef, whereas without the lipid moiety, the N-terminal residues remain flexible (19). Such closed conformation would be in agreement with the sound solubility of myristoylated Nef and its large cytosolic fraction found in transfected cells (11–15,19). Accordingly, this would imply the presence of a lipid-binding site on Nef that recognizes its myristate. When associated to membranes, this lipid recognition site may interact with hydrophobic residues as the dileucine-based sorting motif of CD4 or other lipids that are released from the bilayer, as suggested here. Even though expression of Nef in mammalian cells does not lead to detectable disruption of membranes, more subtle destabilization processes might alter the properties of the host plasma membranes. Of note, we recently identified that the HIV-1 Nef protein modulates the lipid composition of virions and host cell membrane microdomains (48). Perturbations within certain regions of a membrane upon interaction with Nef could at least contribute to such changes in lipid composition and might directly impact on signal transduction processes emanating from these domains or affect their lateral mobility.

SUPPORTING MATERIAL

Four figures and a table are available at http://www.biophysj.org/biophysj/supplemental/S0006-3495(09)00469-X.

Support by the Deutsche Forschungsgemeinschaft (GE-976/1, TR 7013) is gratefully acknowledged.

REFERENCES

1. Geyer, M., O. T. Fackler, and B. M. Peterlin. 2001. Structure-function relationships in HIV-1 Nef. *EMBO Rep.* 2:580–585.
2. Piguet, V., and D. Trono. 1999. The Nef protein of primate lentiviruses. *Rev. Med. Virol.* 9:111–120.
3. Arora, V. K., B. L. Fredericksen, and J. V. Garcia. 2002. Nef: agent of cell subversion. *Microbes Infect.* 4:189–199.
4. Fackler, O. T., and A. S. Baur. 2002. Live and let die: Nef functions beyond HIV replication. *Immunity.* 16:493–497.
5. Roeth, J. F., and K. L. Collins. 2006. Human immunodeficiency virus type 1 Nef: adapting to intracellular trafficking pathways. *Microbiol. Mol. Biol. Rev.* 70:548–563.
6. Fackler, O. T., A. Alcover, and O. Schwartz. 2007. Modulation of the immunological synapse: a key to HIV-1 pathogenesis? *Nat. Rev. Immunol.* 7:310–317.
7. Kestler 3rd, H. W., D. J. Ringler, K. Mori, D. L. Panicali, P. K. Sehgal, et al. 1991. Importance of the nef gene for maintenance of high virus loads and for development of AIDS. *Cell.* 65:651–662.
8. Deacon, N. J., A. Tsykin, A. Solomon, K. Smith, M. Ludford-Menting, et al. 1995. Genomic structure of an attenuated quasi species of HIV-1 from a blood transfusion donor and recipients. *Science.* 270:988–991.
9. Kirchhoff, F., T. C. Greenough, D. B. Brettler, J. L. Sullivan, and R. C. Desrosiers. 1995. Absence of intact nef sequences in a long-term survivor with nonprogressive HIV-1 infection. *N. Engl. J. Med.* 332:228–232.
10. Kaminchik, J., R. Margalit, S. Yaish, H. Drummer, B. Amit, et al. 1994. Cellular distribution of HIV type 1 Nef protein: identification of domains in Nef required for association with membrane and detergent-insoluble cellular matrix. *AIDS Res. Hum. Retroviruses.* 10:1003–1010.
11. Niederman, T. M. J., W. Randall Hastings, and L. Ratner. 1993. Myristoylation-enhanced binding of the HIV-1 Nef protein to T cell skeletal matrix. *Virology.* 197:420–425.
12. Coates, K., S. J. Cooke, D. A. Mann, and M. P. G. Harris. 1997. Protein kinase C-mediated phosphorylation of HIV-1 nef in human cell lines. *J. Biol. Chem.* 272:12289–12294.
13. Fackler, O. T., N. Kienzle, E. Kremmer, A. Boese, B. Schramm, et al. 1997. Association of human immunodeficiency virus Nef protein with actin is myristoylation dependent and influences its subcellular localization. *Eur. J. Biochem.* 247:843–851.
14. Bentham, M., S. Mazaleyrat, and M. Harris. 2006. Role of myristoylation and N-terminal basic residues in membrane association of the human immunodeficiency virus type 1 Nef protein. *J. Gen. Virol.* 87:563–571.
15. Giese, S. I., I. Woerz, S. Homann, N. Triboni, M. Geyer, et al. 2006. Specific and distinct determinants mediate membrane binding and lipid raft incorporation of HIV-1 (SF2). *Nef. J. Virol.* 78:4085–4097.
16. Arold, S. T., and A. S. Baur. 2001. Dynamic Nef and Nef dynamics: how structure could explain the complex activities of this small HIV protein. *Trends Biochem. Sci.* 26:356–363.
17. Murray, D., L. Hermida-Matsumoto, C. A. Buser, J. Tsang, C. T. Sigal, et al. 1998. Electrostatics and the membrane association of Src: theory and experiment. *Biochemistry.* 37:2145–2159.
18. Yalovsky, S., M. Rodr Guez-Concepcion, and W. Gruissem. 1999. Lipid modifications of proteins - slipping in and out of membranes. *Trends Plant Sci.* 4:439–445.
19. Breuer, S., H. Gerlach, B. Kolaric, C. Urbanke, N. Opitz, et al. 2006. Biochemical indication for myristoylation-dependent conformational changes in HIV-1 Nef. *Biochemistry.* 45:2339–2349.
20. Mayer, L. D., M. J. Hope, and P. R. Cullis. 1986. Vesicles of variable size produced by a rapid extrusion procedure. *Biochim. Biophys. Acta.* 858:161–168.
21. Reimhult, E., M. Zach, F. Hook, and B. Kasemo. 2006. A multitechnique study of liposome adsorption on Au and lipid bilayer formation on SiO_2. *Langmuir.* 22:3313–3319.
22. Pfeiffer, I., B. Seantier, S. Petronis, D. Sutherland, B. Kasemo, et al. 2008. Influence of nanotopography on phospholipid bilayer formation on silicon dioxide. *J. Phys. Chem. B.* 112:5175–5181.

23. Keller, C. A., K. Glasmastar, V. P. Zhdanov, and B. Kasemo. 2000. Formation of supported membranes from vesicles. *Phys. Rev. Lett.* 84:5443–5446.

24. Reiter, R., H. Motschmann, H. Orendi, A. Nemetz, and W. Knoll. 1992. Ellipsometric microscopy. Imaging monomolecular surfactant layers at the air-water interface. *Langmuir.* 8:1784–1788.

25. Azzam, R. M. A., and N. M. Bashara. 1999. Ellipsometry and Polarized Light. Elsevier, Amsterdam.

26. Vedam, K. 1998. Spectroscopic ellipsometry: a historical overview. *Thin Solid Films.* 313–314, 1–9.

27. Jin, G., R. Jansson, and H. Arwin. 1996. Imaging ellipsometry revisited: developments for visualization of thin transparent layers on silicon substrates. *Rev. Sci. Instrum.* 67:2930–2936.

28. Alexander, M., Y. C. Bor, K. S. Ravichandran, M. L. Hammarskjold, and D. Rekosh. 2004. Human immunodeficiency virus type I Nef associates with lipid rafts to downmodulate cell surface CD4 and class I major histocompatibility complex expression and to increase viral infectivity. *J. Virol.* 78:1685–1696.

29. Wang, J. K., E. Kiyokawa, E. Verdin, and D. Trono. 2000. The Nef protein of HIV-1 associates with rafts and primes T cells for activation. *Proc. Natl. Acad. Sci. USA.* 97:394–399.

30. Zheng, Y. H., A. Plemenitas, T. Linnemann, O. T. Fackler, and B. M. Peterlin. 2001. Nef increases infectivity of HIV via lipid rafts. *Curr. Biol.* 11:876–879.

31. Schwarz, G., and C. H. Robert. 1990. Pore formation kinetics in membranes, determined from the release of marker molecules out of liposomes or cells. *Biophys. J.* 58:577–583.

32. Schwarz, G., R. T. Zong, and T. Popescu. 1992. Kinetics of melittin induced pore formation in the membrane of lipid vesicles. *Biochim. Biophys. Acta.* 1110:97–104.

33. Rex, S., and G. Schwarz. 1998. Quantitative studies on the melittin-induced leakage mechanism of lipid vesicles. *Biochemistry.* 37:2336–2345.

34. Arbuzova, A., and G. Schwarz. 1999. Pore-forming action of mastoparan peptides on liposomes: a quantitative analysis. *Biochim. Biophys. Acta.* 1420:139–152.

35. Curtain, C. C., F. Separovic, D. Rivett, A. Kirkpatrick, A. J. Waring, et al. 1994. Fusogenic activity of amino-terminal region of HIV type 1 Nef protein. *AIDS Res. Hum. Retroviruses.* 10:1231–1240.

36. Fujii, Y., K. Otake, M. Tashiro, and A. Adachi. 1996. Human immunodeficiency virus type 1 Nef protein on the cell surface is cytocidal for human CD4+ T cells. *FEBS Lett.* 393:105–108.

37. Macreadie, I. G., R. Fernley, L. A. Castelli, A. Lucantoni, J. White, et al. 1998. Expression of HIV-1 nef in yeast causes membrane perturbation and release of the myristylated Nef protein. *J. Biomed. Sci.* 5:203–210.

38. Macreadie, I. G., M. G. Lowe, C. C. Curtain, D. Hewish, and A. A. Azad. 1997. Cytotoxicity resulting from addition of HIV-1 Nef N-terminal peptides to yeast and bacterial cells. *Biochem. Biophys. Res. Commun.* 232:707–711.

39. Barnham, K. J., S. A. Monks, M. G. Hinds, A. A. Azad, and R. S. Norton. 1997. Solution structure of a polypeptide from the N terminus of the HIV protein Nef. *Biochemistry.* 36:5970–5980.

40. Aiken, C., J. Konner, N. R. Landau, M. E. Lenburg, and D. Trono. 1994. Nef induces CD4 endocytosis: requirement for a critical dileucine motif in the membrane-proximal CD4 cytoplasmic domain. *Cell.* 76:853–864.

41. Harris, M. 1995. The role of myristoylation in the interactions between human immunodeficiency virus type I Nef and cellular proteins. *Biochem. Soc. Trans.* 23:557–561.

42. Fackler, O. T., A. Moris, N. Triboni, S. I. Giese, B. Glass, et al. 2006. Functional characterization of HIV-1 Nef mutants in the context of viral infection. *Virology.* 351:322–339.

43. Murray, D., N. Ben-Tal, B. Honig, and S. McLaughlin. 1997. Electrostatic interaction of myristoylated proteins with membranes: simple physics, complicated biology. *Structure.* 5:985–989.

44. Peitzsch, R. M., and S. McLaughlin. 1993. Binding of acylated peptides and fatty acids to phospholipid vesicles: pertinence to myristoylated proteins. *Biochemistry.* 32:10436–10443.

45. Welker, R., M. Harris, B. Cardel, and H.-G. Kräusslich. 1998. Virion incorporation of human immunodeficiency virus type 1 Nef is mediated by a bipartite membrane-targeting signal: analysis of its role in enhancement of viral infectivity. *J. Virol.* 72:8833–8840.

46. Geyer, M., C. E. Munte, J. Schorr, R. Kellner, and H. R. Kalbitzer. 1999. Structure of the anchor-domain of myristoylated and non-myristoylated HIV-1 Nef protein. *J. Mol. Biol.* 289:123–138.

47. Baur, A. S., G. Sass, B. Laffert, D. Willbold, C. Cheng-Mayer, et al. 1997. The N-terminus of Nef from HIV-1/SIV associates with a protein complex containing Lck and a serine kinase. *Immunity.* 6:283–291.

48. Brügger, B., E. Krautkrämer, N. Tibroni, C. E. Munte, S. Rauch, et al. 2007. Human immunodeficiency virus type 1 Nef protein modulates the lipid composition of virions and host cell membrane microdomains. *Retrovirology.* 4:70–82.